© 2018. Published by The Company of Biologists Ltd | Development (2018) 145, dev171827. doi:10.1242/dev.171827

RESEARCH ARTICLE

TBX2 and TBX3 act downstream of canonical WNT signaling in patterning and differentiation of the mouse ureteric mesenchyme

Nurullah Aydoğdu[1], Carsten Rudat[1], Mark-Oliver Trowe[1], Marina Kaiser[1], Timo H. Lüdtke[1], Makoto Mark Taketo[2], Vincent M. Christoffels[3], Anne Moon[4,5] and Andreas Kispert[1,*]

ABSTRACT

The organized array of smooth muscle cells (SMCs) and fibroblasts in the walls of visceral tubular organs arises by patterning and differentiation of mesenchymal progenitors surrounding the epithelial lumen. Here, we show that the TBX2 and TBX3 transcription factors have novel and required roles in regulating these processes in the murine ureter. Co-expression of TBX2 and TBX3 in the inner mesenchymal region of the developing ureter requires canonical WNT signaling. Loss of TBX2/TBX3 in this region disrupts activity of two crucial drivers of the SMC program, *Foxf1* and BMP4 signaling, resulting in decreased SMC differentiation and increased extracellular matrix. Transcriptional profiling and chromatin immunoprecipitation experiments revealed that TBX2/TBX3 directly repress expression of the WNT antagonists *Dkk2* and *Shisa2*, the BMP antagonist *Bmper* and the chemokine *Cxcl12*. These findings suggest that TBX2/TBX3 are effectors of canonical WNT signaling in the ureteric mesenchyme that promote SMC differentiation by maintaining BMP4 and WNT signaling in the inner region, while restricting CXCL12 signaling to the outer layer of fibroblast-fated mesenchyme.

KEY WORDS: Wnt signaling, Differentiation, Mouse, Smooth muscle cell, Ureter

INTRODUCTION

Tubes are fundamental structures in organs that engage in the transport of gases, fluids and solids in metazoans. Besides the luminal epithelial lining, they are characterized by outer layers of fibro-muscular material that provide rigidity, flexibility and contractile activity to the tube (Iruela-Arispe and Beitel, 2013). The mammalian ureters are straight tubes that propel urine from the renal pelvis to the urinary bladder, and represent a simple system in which to analyze molecular pathways that control the differentiation and organization of fibroblasts and smooth muscle cells (SMCs) from a pool of mesenchymal progenitors.

In the mouse, these progenitors are first identified at embryonic day (E) 11.5 as a group of *Tbx18*-expressing fibroblast-like cells that surround the stalk region of the ureteric bud, an epithelial outgrowth of the nephric duct (Airik et al., 2006). At E12.5, *Tbx18*$^{+}$ cells in proximity to the epithelium [hereafter referred to as cells of the inner layer of the ureteric mesenchyme (UM)] acquire a rhomboid shape and are densely compacted. They initiate the SMC program at E14.5 as evidenced by expression of the SMC regulatory gene *Myocd*. The majority of these SMC progenitors become terminally differentiated, contractile SMCs but some regain a fibroblast-like character and populate the subepithelial space. *Tbx18*$^{+}$ cells further distal to the epithelium (hereafter referred to as cells of the outer layer of the UM) maintain their initial fibroblast-like character and differentiate from E13.5 on into adventitial fibroblasts (Bohnenpoll et al., 2017a). Shortly after onset of urine production in the kidney at E16.5, the ureteric wall has acquired a three-layered organization: the fibrous *lamina propria* on the inside, the peristaltically active *tunica muscularis* in the middle, and the fibrous *tunica adventitia* on the outside (Velardo, 1981) (Fig. S1, for a scheme of ureter development).

Tissue recombination and genetic experiments indicate that survival, patterning and differentiation of UM progenitors depend on SHH and WNT signals from the adjacent ureteric epithelium (UE) (Baskin et al., 1996; Bohnenpoll and Kispert, 2014; Cunha et al., 1991; Trowe et al., 2012; Yu et al., 2002). At E11.5, SHH activates a SMO-dependent pathway in the UM that is required for survival of cells in the outer layer, for proliferation and SMC differentiation of cells of the inner layer, and also for urothelial proliferation and differentiation. The proliferation and differentiation functions of SHH signaling are mediated by the forkhead transcription factor FOXF1, which, in turn, induces expression of and synergizes with BMP4 in SMC differentiation (Bohnenpoll et al., 2017b; Mamo et al., 2017). At E12.5, WNT7B and WNT9B activate the canonical WNT pathway in cells of the inner mesenchymal layer, disruption of which results in reduced proliferation and failed SMC differentiation of these cells, and expansion of the adventitial fate to the inner layer (Trowe et al., 2012). The transcription factors that mediate WNT signaling downstream of β-catenin (CTNNB1) in the UM are unknown.

Tbx2 and *Tbx3* are two closely related members of the evolutionarily conserved family of T-box transcription factor genes (Papaioannou, 2014). Both encode transcriptional repressors that regulate proliferation, patterning and differentiation programs in a variety of developmental contexts, in some cases redundantly (Douglas and Papaioannou, 2013; Lu et al., 2010; Lüdtke et al., 2016; Singh et al., 2012; Zirzow et al., 2009).

Expression of *TBX2* in the human fetal and adult kidney (Campbell et al., 1995; Law et al., 1995), of *Tbx3* in the bladder urothelium (Ito et al., 2005), of *Tbx2* and *Tbx3* in the nephric duct and in the mesenchymal core of the developing urethra in the mouse (Chapman et al., 1996; Douglas et al., 2012), and urinary tract abnormalities in human patients with heterozygous loss of *TBX3* (Gonzalez et al., 1976; Pallister et al., 1976) indicate that both genes

[1]Institut für Molekularbiologie, Medizinische Hochschule Hannover, 30625 Hannover, Germany. [2]Division of Experimental Therapeutics, Graduate School of Medicine, Kyoto University, Kyoto 606-8501, Japan. [3]Department of Anatomy, Embryology and Physiology, Academic Medical Center, University of Amsterdam, 1105 AZ Amsterdam, The Netherlands. [4]Department of Molecular and Functional Genomics, Weis Center for Research, Geisinger Clinic, Danville PA 17822, USA. [5]Departments of Pediatrics and Human Genetics, University of Utah School of Medicine, Salt Lake City, UT 84112, USA.

*Author for correspondence (kispert.andreas@mh-hannover.de)

A.K., 0000-0002-8154-0257

Received 12 September 2018; Accepted 24 October 2018

Development (2018) 145, dev171827. doi:10.1242/dev.171827

also contribute to multiple subprograms in the development of different organs of the mammalian urinary tract. Here, we demonstrate essential roles for these factors in the differentiation of the mesenchymal components of the mouse ureter. We show that both genes are expressed in the inner layer of the UM in a *Ctnnb1*-dependent manner, and that they mediate a subset of canonical WNT signals in this tissue.

RESULTS

Tbx2 and *Tbx3* expression in the UM depends on canonical WNT signaling

To determine the expression of *Tbx2* and *Tbx3* in ureter development, we performed *in situ* hybridization analysis on transverse sections of the trunk region of E12.5-E18.5 wild-type embryos. At all stages, *Tbx2* and *Tbx3* transcripts were abundant in the epithelial compartment of the ureter and also present in adjacent mesenchymal cells both at the proximal (kidney) level (Fig. 1A) as well as distally, i.e. close to the bladder (Fig. S2A). Immunofluorescence analysis confirmed expression of TBX2 and TBX3 protein in the UE from E12.5 to E18.5. Expression in the UM was prominent at E12.5 and E14.5, and weaker at E16.5 (Fig. 1B; Fig. S2B).

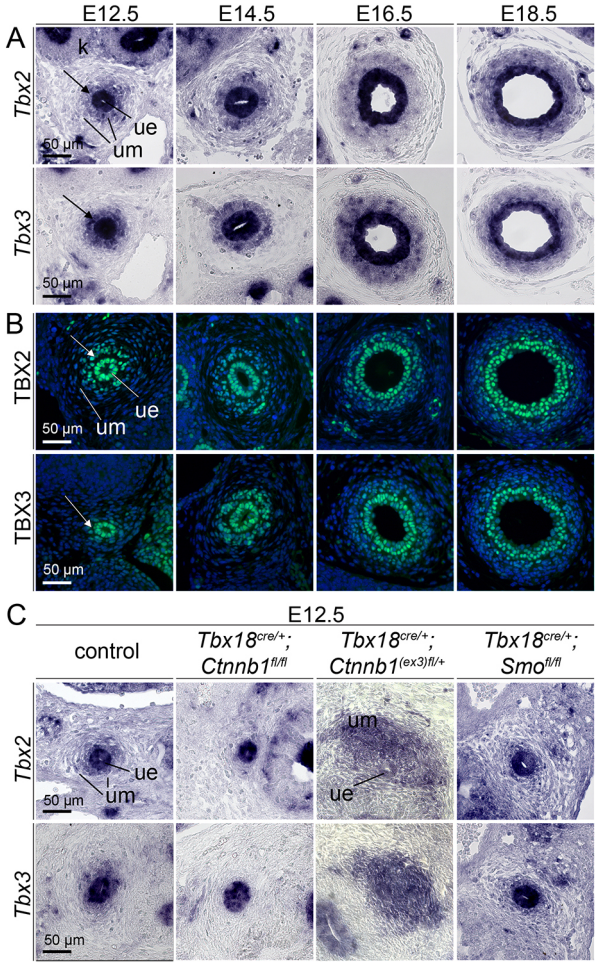

Fig. 1. Expression of *Tbx2* and *Tbx3* during embryonic ureter development. (A,B) RNA *in situ* hybridization (A) and immunofluorescence analysis (B) on transverse sections through the posterior trunk region of wild-type embryos at the proximal (kidney) level of the ureter. Arrows point to the mesenchymal expression domain in E12.5 ureters. Nuclei (blue) are counterstained with DAPI in B. (C) Comparative RNA *in situ* hybridization analysis on transverse sections through the posterior trunk region of E12.5 wild-type embryos, of embryos with loss of *Ctnnb1*-dependent WNT signaling (*Tbx18*$^{cre/+}$;*Ctnnb1*$^{fl/fl}$), with gain of *Ctnnb1*-dependent WNT signaling (*Tbx18*$^{cre/+}$;*Ctnnb1*$^{(ex3)fl/+}$) and loss of SHH/SMO signaling (*Tbx18*$^{cre/+}$;*Smo*$^{fl/fl}$) in the UM. k, kidney; ue, ureteric epithelium; um, ureteric mesenchyme.

Because expression of both genes was restricted to the inner layer of the UM, we questioned whether their expression depends on SHH or WNT signals emanating from the UE (Trowe et al., 2012; Yu et al., 2002). To address this question, we used a conditional pathway deletion approach, with a *Tbx18*^{cre} line, which mediates recombination in the entire UM starting from E11.5 (Airik et al., 2010; Bohnenpoll et al., 2013), and floxed alleles of the unique mediator of SHH signaling, *Smo* (Long et al., 2001), and of canonical WNT signaling, *Ctnnb1* (Brault et al., 2001), as previously reported (Bohnenpoll et al., 2017b; Trowe et al., 2012). Loss of *Smo* had no effect on *Tbx2* and *Tbx3* expression in the UM at E12.5 (Fig. 1C). In contrast, expression of both genes was lost from this region in *Tbx18*$^{cre/+}$;*Ctnnb1*$^{fl/fl}$ embryos. Moreover, misexpression of a stabilized version of CTNNB1 in the entire UM (mimicking activated WNT signaling; *Tbx18*$^{cre/+}$;*Ctnnb1*$^{ex3(fl)/+}$) (Harada et al., 1999; Trowe et al., 2012) resulted in increased and expanded expression of *Tbx2* and *Tbx3* in this region at E12.5 (Fig. 1C). Together, this analysis indicates that expression of *Tbx2* and *Tbx3* in the inner layer of the UM depends on canonical WNT signaling and is independent of the SHH pathway.

Loss of *Tbx2* and *Tbx3* in the UM leads to reduced SMC differentiation

To investigate the role of *Tbx2* and *Tbx3* in the UM, we used the *Tbx18*^{cre} line and floxed alleles of *Tbx2* (Wakker et al., 2010) and *Tbx3* (Frank et al., 2013). The validity of this approach was confirmed by absence of TBX2 and TBX3 protein expression specifically in the mesenchymal compartment of *Tbx18*$^{cre/+}$;*Tbx2*$^{fl/fl}$;*Tbx3*$^{fl/fl}$ (*Tbx2/3cDKO*) ureters at E12.5 (Fig. S3).

At E18.5, whole-mount preparations of urogenital systems of mice with conditional loss of two or three alleles of *Tbx2* and/or *Tbx3* appeared grossly normal (Fig. S4A). Kidneys and ureters were histologically undistinguishable from the controls (Fig. S4B). Expression of the SMC regulatory gene *Myocd* and of the SMC structural genes *Myh11*, *Tagln* and *Tnnt2* was normal or appeared slightly reduced (*Tnnt2* in the *Tbx2* and *Tbx3* single mutants). The adventitial marker genes *Col1a2*, *Fbln2* and *Dpt*, and the *lamina propria* marker *Aldh1a2* were normally expressed in the mutants (Fig. S4C), arguing that patterning of the mesenchymal compartment of the ureter is undisturbed, and SMC differentiation is minimally affected in triple allele mutants.

We next analyzed compound homozygous double mutants. At E18.5, urogenital systems of *Tbx2/3cDKO* embryos appeared morphologically unaffected (Fig. 2A). We did not detect histological changes in the kidney, but the mutant ureter lacked a clear distinction between a condensed inner and a more loosely organized outer mesenchymal layer. Instead, the entire UM was loosely organized with excessive extracellular space (Fig. 2B). Expression of SMC markers (*Myocd*, *Myh11*, *Tagln*, *Tnnt2*) was reduced to small patches of cells. The *lamina propria* marker *Aldh1a2* was restricted to a cell layer directly underneath the epithelium, as in the control. Some markers of the outer adventitial layer appeared unchanged (*Dpt*, *Postn*) whereas others were strongly expanded to the inner mesenchymal region (*Col1a1*, *Col1a2*, *Fbln2*) (Fig. 2C). Differentiation of urothelial cell types was unaffected in the mutant as revealed by normal expression of KRT5, ΔNP63 and UPK1B, which combinatorially marked basal cells (KRT5^{+}ΔNP63^{+}UPK1B^{-}), intermediate cells

Development (2018) 145, dev171827. doi:10.1242/dev.171827

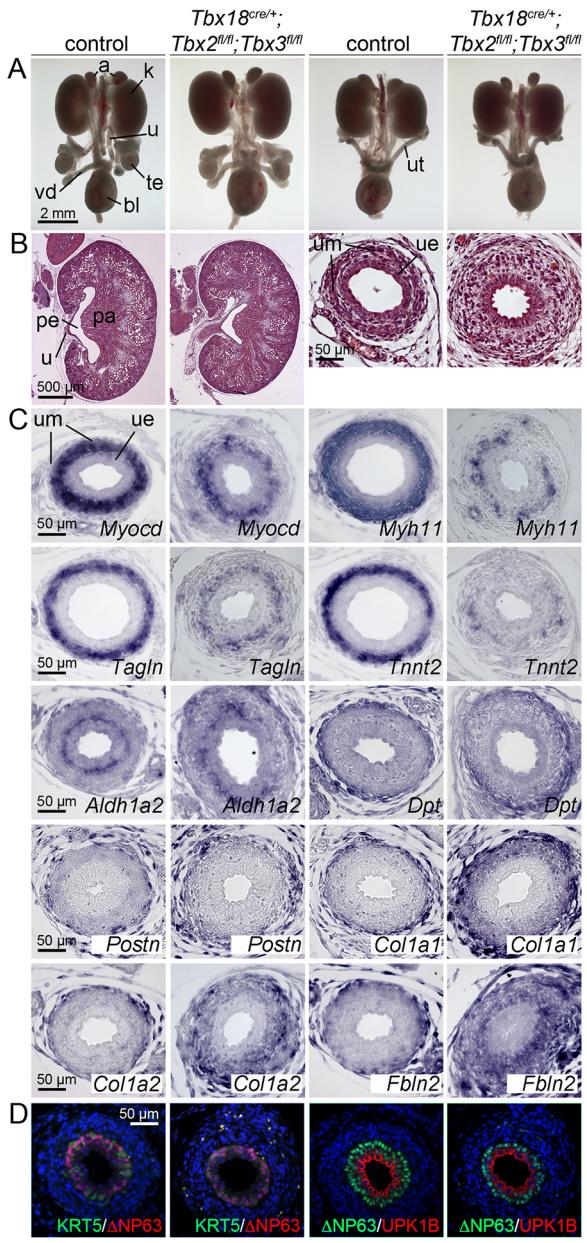

Fig. 2. Ureter anomalies in *Tbx18*$^{cre/+}$;*Tbx2*$^{fl/fl}$;*Tbx3*$^{fl/fl}$ embryos at E18.5. (A) Morphology of whole urogenital systems of male (column 1 and 2) and female (column 3 and 4) embryos. $n \geq 5$, all groups. (B) Hematoxylin and Eosin staining of sagittal sections of kidneys (column 1 and 2) and of transverse sections of the proximal ureter (column 3 and 4). Note the dispersed nature of the mesenchymal cells in the mutant ureter. (C) RNA *in situ* hybridization analysis on transverse sections of the proximal ureter for SMC markers (*Myocd*, *Myh11*, *Tagln*, *Tnnt2*), the *lamina propria* marker *Aldh1a2*, and adventitial markers (*Dpt*, *Postn*, *Col1a1*, *Col1a2*, *Fbln2*). (D) Analysis of urothelial differentiation by immunofluorescence of KRT5, ΔNP63 and UPK1B; nuclei (blue) are counterstained with DAPI. a, adrenal; bl, bladder; k, kidney; pa, papilla; pe, pelvis; te, testis; u, ureter; ue, ureteric epithelium; um, ureteric mesenchyme; ut, uterus; vd, vas deferens.

(KRT5^{-}ΔNP63^{+}UPK1B^{+}) and superficial cells (KRT5^{-}ΔNP63^{-}UPK1B^{+}) (Fig. 2D) (Bohnenpoll et al., 2017a).

To profile the molecular and cellular changes in E18.5 *Tbx2/3cDKO* ureters in an unbiased fashion, we compared their transcriptome with that of control ureters by microarray analysis. Using a threshold of 1.5-fold change and an expression intensity robustly above background (>100), we detected 405 genes with reduced expression and 327 with increased expression in *Tbx2/3cDKO* ureters (Fig. 3A; Tables S1, S2). Functional annotation using the DAVID software tool revealed strong enrichment of the terms extracellular matrix (ECM) and collagen in the pool of upregulated genes whereas the pool of downregulated genes was strongly enriched for various terms relating to structure and function of SMCs (Fig. 3B,C; Tables S3, S4). Hence, loss of *Tbx2* and *Tbx3* in the UM leads to a reduced SMC phenotype and a gain of ECM (mostly collagen and fibulin) deposition in the inner layer.

Loss of *Tbx2* and *Tbx3* in the UM disrupts ureter peristalsis

Tbx2/3cDKO ureters did not present the dilatation phenotype described in other mutants with reduced SMC investment (Bohnenpoll et al., 2017b; Mamo et al., 2017; Trowe et al., 2012), so we questioned whether peristalsis was affected. We isolated E18.5 ureters and cultured them for 6 days in a transwell setting, monitoring contraction frequency and intensity daily (Fig. 3D-F). After 1 day of culture both wild-type and mutant ureters contracted approximately three times per minute. Whereas the contraction frequency of the wild-type ureters decreased to 1.3 at day 6, that of mutant ureters increased to 4.6 (Fig. 3E). Interestingly, the contraction intensity of mutant ureters was significantly lower at all analyzed time points (Fig. 3F; Movies 1, 2). Together, this argues that reduced SMC investment results in reduced contraction intensity, which is counteracted by an increased contraction frequency, thus preventing dilatation at least up to this stage.

Early onset of ureter defects in *Tbx2/3cDKO* embryos

To define both the onset as well as the progression of mesenchymal defects in *Tbx2/3cDKO* ureters, we analyzed earlier embryonic stages. Histological analysis revealed a clear division of the UM into an inner layer with rhomboid-shaped condensed cells and an outer layer with loosely organized fibroblast-like cells at E14.5, E15.5 and E16.5 in the wild type. In the mutant, the UM was similarly subdivided at E14.5 but the inner layer appeared progressively less condensed at the subsequent stages (Fig. 4A). In the wild type, onset of *Myocd* expression at E14.5 was followed by that of *Myh11*, *Tagln* and *Tnnt2* 1 day later (Fig. 4B). *Col1a2* and *Fbln2* expression was homogeneous in the UM at E14.5, but was downregulated in the inner layer at E16.5. In the mutant ureter, *Myocd* and SMC structural genes were not activated until E16.5 and then only weakly. In contrast, *Col1a2* and *Fbln2* expression was found throughout the mutant UM at all stages (Fig. 4C). This SMC differentiation defect was accompanied by a delayed onset of peristaltic activity. Wild-type ureters explanted at E14.5 commenced contractions after 2 days in culture whereas mutant ureters started to contract after 4-6 days and had reduced contraction intensity and SMC investment (Fig. 4D,E; Fig. S5; Movies 3, 4).

A terminal deoxynucleotidyl transferase dUTP nick end labeling (TUNEL) assay did not detect apoptotic cells at E12.5 and at E14.5 in the mutant UM nor did a 5-bromo-2′-deoxyuridine (BrdU) incorporation assay reveal changes of proliferation in this tissue or the adjacent epithelium indicating that delayed SMC differentiation is not due to changes in either of these cellular programs (Fig. S6).

Reduced activity of a *Foxf1*-BMP4 module precedes SMC differentiation defects

To identify the molecular causes of the SMC differentiation defect and the de-repression of ECM genes in the inner layer of the UM in *Tbx2/3cDKO* embryos, we screened expression of a panel of

Development (2018) 145, dev171827. doi:10.1242/dev.171827

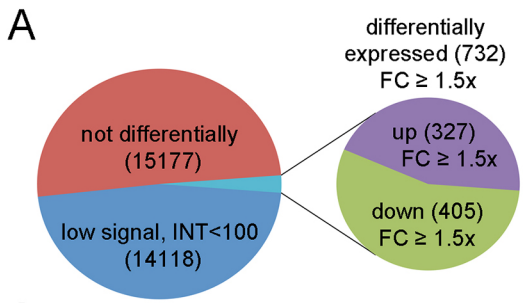

B

Top 15 enriched functional annotations for upregulated genes (DAVID,david.ncifcrf.gov)

Term	Category	p value	Fold Enrichment
Glycoprotein	UP_KEYWORDS	4.10E-21	2.3
Extracellular matrix	UP_KEYWORDS	3.97E-20	9.3
Signal	UP_KEYWORDS	1.89E-19	2.2
proteinaceous extracellular matrix	GOTERM_CC_DIRECT	2.11E-19	7.3
extracellular matrix	GOTERM_CC_DIRECT	2.28E-19	9.6
Secreted	UP_KEYWORDS	8.02E-19	3.1
Disulfide bond	UP_KEYWORDS	1.10E-18	2.4
extracellular region	GOTERM_CC_DIRECT	1.05E-15	2.8
Developmental protein	UP_KEYWORDS	1.19E-11	3.2
Hydroxylation	UP_KEYWORDS	2.43E-11	12.0
collagen trimer	GOTERM_CC_DIRECT	2.14E-10	11.5
Collagen	UP_KEYWORDS	2.46E-10	11.4
multicellular organismal development	GOTERM_BP_DIRECT	2.70E-10	2.9
collagen fibril organization	GOTERM_BP_DIRECT	3.82E-10	17.6
cell adhesion	GOTERM_BP_DIRECT	1.88E-09	3.9

Top 15 enriched functional annotations for downregulated genes (DAVID,david.ncifcrf.gov)

Term	Category	p value	Fold Enrichment
Muscle protein	UP_KEYWORDS	1.10E-24	26.5
Z disc	GOTERM_CC_DIRECT	1.41E-18	13.4
sarcolemma	GOTERM_CC_DIRECT	3.50E-12	9.8
Hypertrophic cardiomyopathy (HCM)	KEGG_PATHWAY	4.12E-10	10.6
actin binding	GOTERM_MF_DIRECT	6.88E-10	4.5
Dilated cardiomyopathy	KEGG_PATHWAY	7.80E-10	10.1
cGMP-PKG signaling pathway	KEGG_PATHWAY	1.74E-09	6.4
Vascular smooth muscle contraction	KEGG_PATHWAY	1.88E-08	7.1
regulation of muscle contraction	GOTERM_BP_DIRECT	2.73E-08	23.3
Actin-binding	UP_KEYWORDS	9.74E-08	4.8
LIM domain	UP_KEYWORDS	2.33E-07	9.4
muscle contraction	GOTERM_BP_DIRECT	2.72E-07	13.4
sarcoplasmic reticulum	GOTERM_CC_DIRECT	3.06E-07	10.8
sarcoplasmic reticulum membrane	GOTERM_CC_DIRECT	3.36E-07	23.1
Adrenergic signaling in cardiomyocytes	KEGG_PATHWAY	1.05E-06	5.6

C

UP_KEYWORDS: Extracellular matrix

Gene	avg FC	Gene	avg FC	Gene	avg FC
Col1a1	2.7	*Col14a1*	1.7	*Lum*	2.1
Col1a2	2.5	*Col16a1*	1.6	*Nid2*	1.6
Col2a1	3.0	*Dcn*	1.9	*Podn*	2.0
Col5a1	2.0	*Fbln1*	2.4	*Smoc1*	1.9
Col6a1	1.7	*Fbln2*	2.1	*Spock2*	1.9
Col8a1	3.1	*Fbln5*	1.9		
Col8a2	1.8	*Fmod*	1.8		
Col9a1	2.1	*Fn1*	2.2		
Col9a2	1.9	*Frem1*	2.2		
Col11a1	1.8	*Lama1*	3.8		
Col12a1	1.9	*Ltbp4*	1.9		

UP_KEYWORDS: Muscle protein

Gene	avg FC	Gene	avg FC
Acta1	-6.5	*Myl6*	-2.2
Acta2	-6.4	*Myl9*	-3.8
Actc1	-5.6	*Myom1*	-9.8
Actg2	-6.7	*Tagln*	-6.7
Casq1	-10.3	*Tnnc1*	-3.7
Casq2	-6.5	*Tnnc2*	-3.9
Des	-3.4	*Tnnt1*	-5.1
Myh11	-6.2	*Tnnt2*	-10.0
Myh6	-21.5	*Tnnt3*	-2.3
Myh8	-1.9	*Tpm1*	-2.6
Myl4	-7.9	*Tpm2*	-4.7

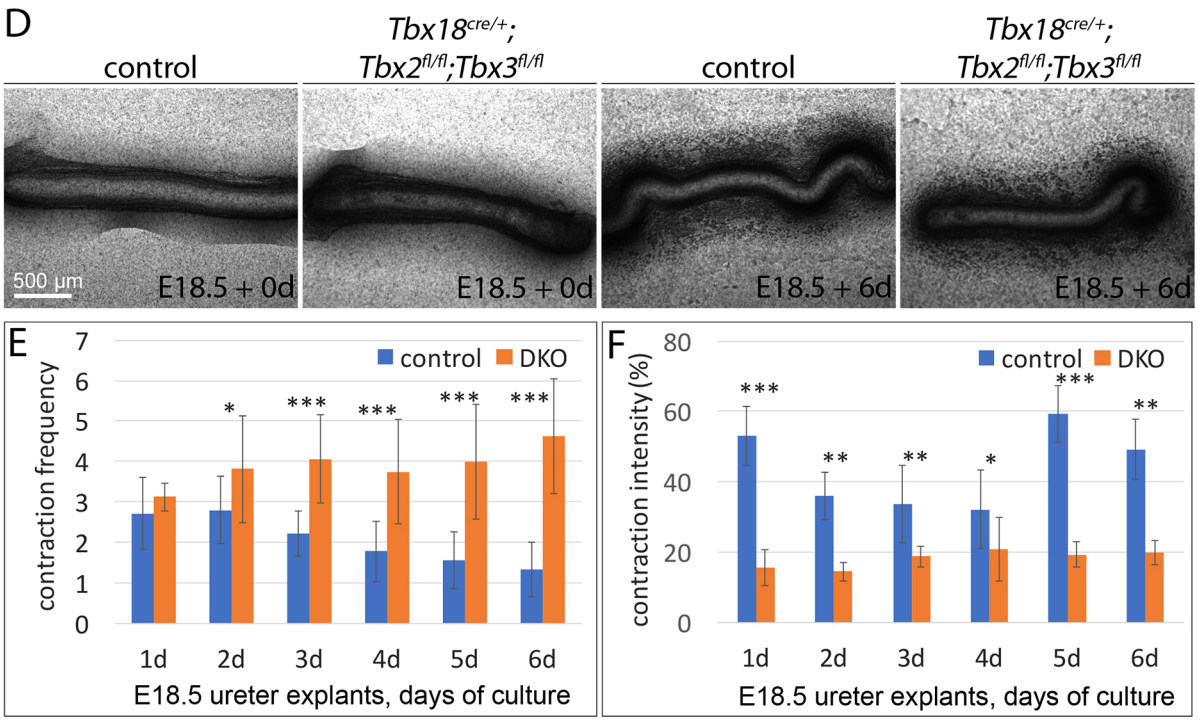

Fig. 3. E18.5 *Tbx18*$^{cre/+}$*;Tbx2*$^{fl/fl}$*;Tbx3*$^{fl/fl}$ ureters show altered cytodifferentiation and peristaltic activity. (A) Pie chart summarizing the results from the microarray analysis of E18.5 wild-type and *Tbx18*$^{cre/+}$*;Tbx2*$^{fl/fl}$*;Tbx3*$^{fl/fl}$ ureters. (B) List of top 15 annotations over-represented in the set of genes upregulated (upper panel) and downregulated (lower panel) in their expression using DAVID web software. (C) Table of transcripts enriched for the terms ECM and collagen in the set of upregulated genes and table of transcripts enriched for the terms SMC and muscle in the set of downregulated genes. (D) Bright-field images of whole ureters explanted from E18.5 embryos and cultured for 0 and 6 days. (E) Contraction frequencies (measured as number of contractions per min) of E18.5 control (blue, *n*=9) and *Tbx18*$^{cre/+}$*;Tbx2*$^{fl/fl}$*;Tbx3*$^{fl/fl}$ ureters (DKO, orange, *n*=4) between day 1 and 6 of culture. Control versus mutant: 1d, 2.7±0.9 versus 3.1±0.4, *P*=0.2; 2d, 2.8±0.8 versus 3.8±1.3, *P*=0.024; 3d, 2.2±0.5 versus 4.1±1.1, *P*=5.4E−06; 4d, 1.8±0.7 versus 3.8±1.3, *P*=4.1E−05; 5d, 1.6±0.7 versus 4.0±1.4, *P*=3.9E−06; 6d, 1.3±0.7 versus 4.6±1.4, *P*=2.5E−08. (F) Contraction intensity (as defined in Materials and Methods) of the same ureters as in E from E18.5 control and *Tbx18*$^{cre/+}$*;Tbx2*$^{fl/fl}$*;Tbx3*$^{fl/fl}$ embryos between day 1 and 6 of culture. Control versus mutant: 1d, 53.2±8.4 versus 15.6±5.2, *P*=3.6E−08; 2d, 36.0±6.7 versus 14.5±2.6, *P*=0.003; 3d, 33.6±11.0 versus 18.7±3.1, *P*=0.002; 4d, 32.1±11.2 versus 20.9±8.9, *P*=0.042; 5d, 59.4±8.0 versus 19.3±3.6, *P*=3.4E−09; 6d, 49.3±8.6 versus 19.9±3.5, *P*=0.001. Data are shown as mean±sd. **P*<0.05; ***P*<0.01; ****P*<0.001; two-tailed Student's *t*-test. FC, fold change; INT, expression intensity.

genes previously implicated in the early development of the UM and the initiation of the SMC program (Bohnenpoll and Kispert, 2014). In E12.5 wild-type ureters, expression of *Ptch1* (target of SHH signaling; Ingham and McMahon, 2001), *Bmp4*, *Axin2* (target of WNT signaling; Jho et al., 2002) and *Rarb* (target of retinoic acid signaling; Mendelsohn et al., 1991), and of the transcription factor genes *Tbx18*, *Sox9*, *Tcf21* and *Tshz3* were expressed in the UM with highest levels in cells adjacent to the epithelium. Expression of all genes appeared unchanged in *Tbx2/3cDKO* ureters (Fig. S7).

Development (2018) 145, dev171827. doi:10.1242/dev.171827

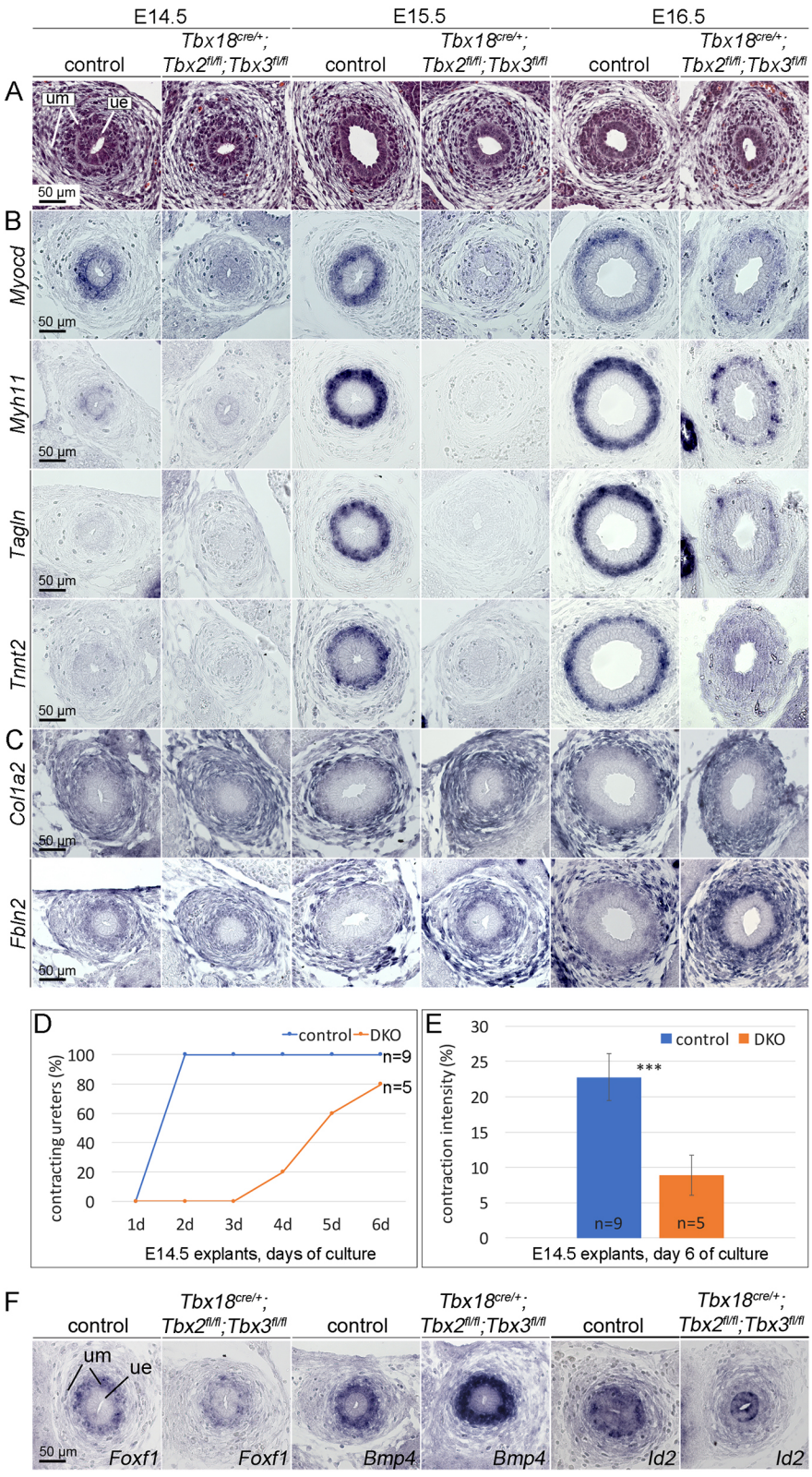

Fig. 4. Onset of SMC differentiation is severely delayed in *Tbx18*$^{cre/+}$;*Tbx2*$^{fl/fl}$;*Tbx3*$^{fl/fl}$ ureters. (A) Hematoxylin and Eosin staining of transverse sections of the proximal ureter at E14.5, E15.5 and E16.5. (B) Cytodifferentiation of SMCs as detected by *in situ* hybridization of marker gene expression on transverse embryo sections is severely delayed in the mutant UM. (C) *In situ* hybridization analysis shows persistent expression of the ECM markers *Col1a2* and *Fbln2* in the UM of mutants after E14.5. (D,E) Analysis of contractions of ureters explanted at E14.5 and cultured for 6 days. Shown are the percentage of ureters [control (blue) *n*=9, mutant (orange, DKO), *n*=5] that have initiated normal proximal to distal contractions at each day of the culture (D), and the contraction intensity of control ureters (22.8±3.4) and mutant ureters (8.9±2.8) after 6 days of culture, *P*=7.3E−08. Data are shown as mean±sd. ***P<0.001; two-tailed Student's *t*-test (E). (F) *In situ* hybridization analysis on transverse sections of the proximal ureter region at E14.5. ue, ureteric epithelium; um, ureteric mesenchyme.

In E14.5 wild-type ureters, the genes listed above and *Id2* (BMP target; Hollnagel et al., 1999) were expressed in SMC progenitors. S*ox9* was an exception as it was decreased. In *Tbx2/3cDKO* ureters, expression of *Ptch1*, *Axin2*, *Rarb*, *Tbx18*, *Tshz3* and *Sox9* was unchanged (Fig. S8). In contrast, *Foxf1* was reduced. Expression of *Bmp4* was strongly increased, whereas its target gene *Id2* showed strongly reduced expression in the UM and unaltered expression in the epithelium (Fig. 4F). Thus, despite increased *Bmp4* expression, the data indicate decreased BMP signaling in the UM. This, in combination with reduced expression of the SMC regulatory gene *Foxf1* (Bohnenpoll et al., 2017b), likely contributes to the delayed and reduced SMC differentiation observed in *Tbx2/3cDKO* ureters.

Development (2018) 145, dev171827. doi:10.1242/dev.171827

Ectopic expression of TBX2 in the UM interferes with mesenchymal patterning and differentiation

Expression of TBX2 and TBX3 is confined to the inner layer of the UM from E12.5 to E16.5. To explore the significance of this temporo-spatial restriction and to gain further insight into the molecular function of these two transcription factors in the UM, we utilized a Cre/loxP-based misexpression approach.

For this, we employed the *Tbx18*^{cre} line, and a *Hprt*^{TBX2} line harboring an integration of a bicistronic transgene-cassette containing the human *TBX2* open-reading frame followed by IRES-GFP in the ubiquitously expressed X-chromosomal *Hprt* locus (Singh et al., 2012). Owing to random X-chromosome inactivation, *Tbx18*$^{cre/+}$;*Hprt*$^{TBX2/+}$ [female gain of function (GOF)] embryos have mosaic TBX2 expression whereas *Tbx18*$^{cre/+}$;*Hprt*$^{TBX2/y}$ (male GOF) embryos expressed the transgene in a uniform manner in the UM (Fig. S9).

Transgene expression did not interfere with viability of embryos at E18.5 but did affect the integrity of the urogenital system. Male GOF embryos invariably developed uretero-pelvic junction obstruction (Fig. 5A-C) and females had bilateral hydroureter with associated hydronephrosis (Fig. S10A-C). Expression of SMC genes was strongly reduced in male and female GOF ureters (Fig. 5D-G; Fig. S10D-G) as was the thickness of the adventitial layer at this stage (Fig. 5H,I; Fig. S10H,I).

Analysis of GOF ureters at E14.5 to E16.5 showed that SMC differentiation was delayed and reduced (Fig. 5J-M; Fig. S10J-M). Markers of the ECM were variably affected: *Col1a2* was minimally affected whereas *Fbln2* was markedly reduced in the outer layer of the UM (Fig. 5N,O; Fig. S10N,O).

Analysis of E14.5 male GOF ureters revealed that ectopic TBX2 did not alter expression of *Ptch1*, *Axin2*, *Bmp4*, *Id2*, *Rarb*, *Tshz3*, *Tbx18* and *Sox9* in the UM (Fig. S11). In contrast, expression of *Foxf1* was markedly decreased; expression of *Postn* and *Foxd1* in the outer layer of the UM was undetectable (Fig. 5P). Hence, ectopic expression of TBX2 interferes with mesenchymal patterning and SMC differentiation in the ureter, as does the combined loss of *Tbx2* and *Tbx3*.

Comparative transcriptome analysis of *Tbx2* loss- and gain-of-function ureters identifies genes regulated by TBX2/TBX3

As *Tbx2* and *Tbx3* often function as transcriptional repressors, many of their target genes should be activated under loss- and repressed under gain-of-function conditions. To identify such genes in an unbiased fashion, we performed microarray-based gene expression profiling. We compared wild-type and *Tbx2/3cDKO* ureters at E14.5, and wild-type and male GOF ureters at E13.5 to obtain a 2-day window of transcriptional changes in both loss- and gain-of-function conditions. Because the inner layer of the UM (where TBX2 and TBX3 function) represents only a fraction of the entire ureter, we employed a relatively low fold-change filter of 1.2. Using an intensity threshold of 100 as additional filter, we identified 238 genes that were consistently upregulated and 260 genes that were downregulated in *Tbx2/3cDKO* ureters (Fig. 6A; Tables S5, S6). Functional annotation found an enrichment of ECM terms with the pool of upregulated genes (Tables S7, S8). In male GOF ureters, expression of 298 genes was down- and of 442 genes upregulated (Fig. 6B; Tables S9, S10). The downregulated transcripts were enriched for the functional annotation terms muscle, ECM and WNT (Tables S11, S12).

The microarrays quantitatively confirmed the results of our *in situ* hybridization analysis of expression of SMC regulatory genes and pathways in the mutant ureters (Fig. 4F and Fig. 5P). Additionally, *Id4*, another direct target of BMP4 signaling (Liu and Harland, 2003), was decreased (−1.5). In male GOF ureters, expression of *Foxf1* was decreased (−1.5) as was that of *Tbx18* (−1.4) (Tables S5, S6, S9, S10).

We found 30 genes at the intersection of upregulated genes in *Tbx2/3cDKO* ureters and downregulated genes in male GOF ureters. Ten of these 30 genes were also upregulated in their expression in the microarray from E18.5 *Tbx2/3cDKO* ureters. *Cxcl12* was slightly below the threshold in the E14.5 *Tbx2/3cDKO* pools (1.2-fold upregulated). We included this gene in the analysis because it was changed in *Ctnnb1*-deficient ureters (Trowe et al., 2012) (Fig. 3A and Fig. 6C,D; Table S13).

We used *in situ* hybridization to validate the expression of these genes in E14.5 control, *Tbx2/3cDKO* and male GOF ureters (Figs S12, S13). We found six genes with differential expression in any two of the three genotypes: *Bmper*, which encodes a BMP antagonist (Moser et al., 2003); *Cxcl12*, which encodes a chemokine (Harris et al., 2013); *Dkk2* and *Shisa2* encoding WNT antagonists (Glinka et al., 1998; Yamamoto et al., 2005); the vascular cell adhesion molecule gene *Vcam1*; and *Fam129a*, a gene without known protein function (Figs S12, S13). In the wild type, *Bmper* and *Cxcl12* were uniformly expressed in the entire UM at E13.5 but subsequently restricted to the outer layer. In *Tbx2/3cDKO* ureters, *Bmper* and *Cxcl12* expression in the inner layer of the UM remained high from E13.5 onwards whereas in GOF ureters it was reduced. *Dkk2* was weakly expressed in the inner region of the UM of E13.5 wild-type embryos but subsequently downregulated. In *Tbx2/3cDKO* ureters, there was ectopic *Dkk2* expression in the inner layer of the UM at E14.5. *Shisa2* expression was confined to this region at E13.5 and E14.5 and expression in *Tbx2/3cDKO* ureters was increased at E14.5 and further augmented at E18.5. In GOF mutants, *Shisa2* expression was reduced at E14.5 (Fig. 6E). *Vcam1* was largely confined to the outer layer of the UM in the wild type. In *Tbx2/3cDKO* embryos, expression was slightly increased in the inner layer of the UM. In male GOF mutants, expression appeared slightly reduced in the entire UM (Fig. S13). Finally, *Fam129a* was expressed in the outer layer of the UM of wild-type embryos at E14.5. Expression in this domain was unaltered in the loss- but decreased in the gain-of-function condition at this stage (Fig. S12).

The expression patterns of *Bmper*, *Cxcl12*, *Dkk2* and *Shisa2* in the *Tbx2/Tbx3* loss- and gain-of function conditions are consistent with these genes being direct targets of TBX2/TBX3-mediated transcriptional repression in the UM. Because embryonic ureters represent a tiny source of chromatin, we did not attempt a genome-wide occupancy chromatin immunoprecipitation (ChIP) experiment. Instead, we interrogated a previously generated data set of TBX3-bound chromatin from the embryonic lung, in which TBX2 and TBX3 are also functional in the undifferentiated mesenchyme (Lüdtke et al., 2016). We found TBX3 binding peaks associated with all four genes (Fig. S14, Table S14).

To validate whether TBX2 binds to genomic sequences harboring these peak regions, we performed ChIP on wild-type E16.5 ureters using anti-TBX2 antibody (Fig. 6F; Table S14). Enrichment was detected for the one peak found in *Shisa2*, and for one of the four and six tested peaks in *Cxcl12* and *Dkk2*, respectively. Multiple peaks were enriched in *Bmper* (Fig. 6F,G). Hence, *Bmper*, *Dkk2*, *Shisa2* and *Cxcl12* may be direct targets of TBX2/TBX3 activity in the UM.

DISCUSSION

TBX2 and TBX3 are members of a closely related subfamily of T-box transcription factors that regulate a diverse array of

Development (2018) 145, dev171827. doi:10.1242/dev.171827

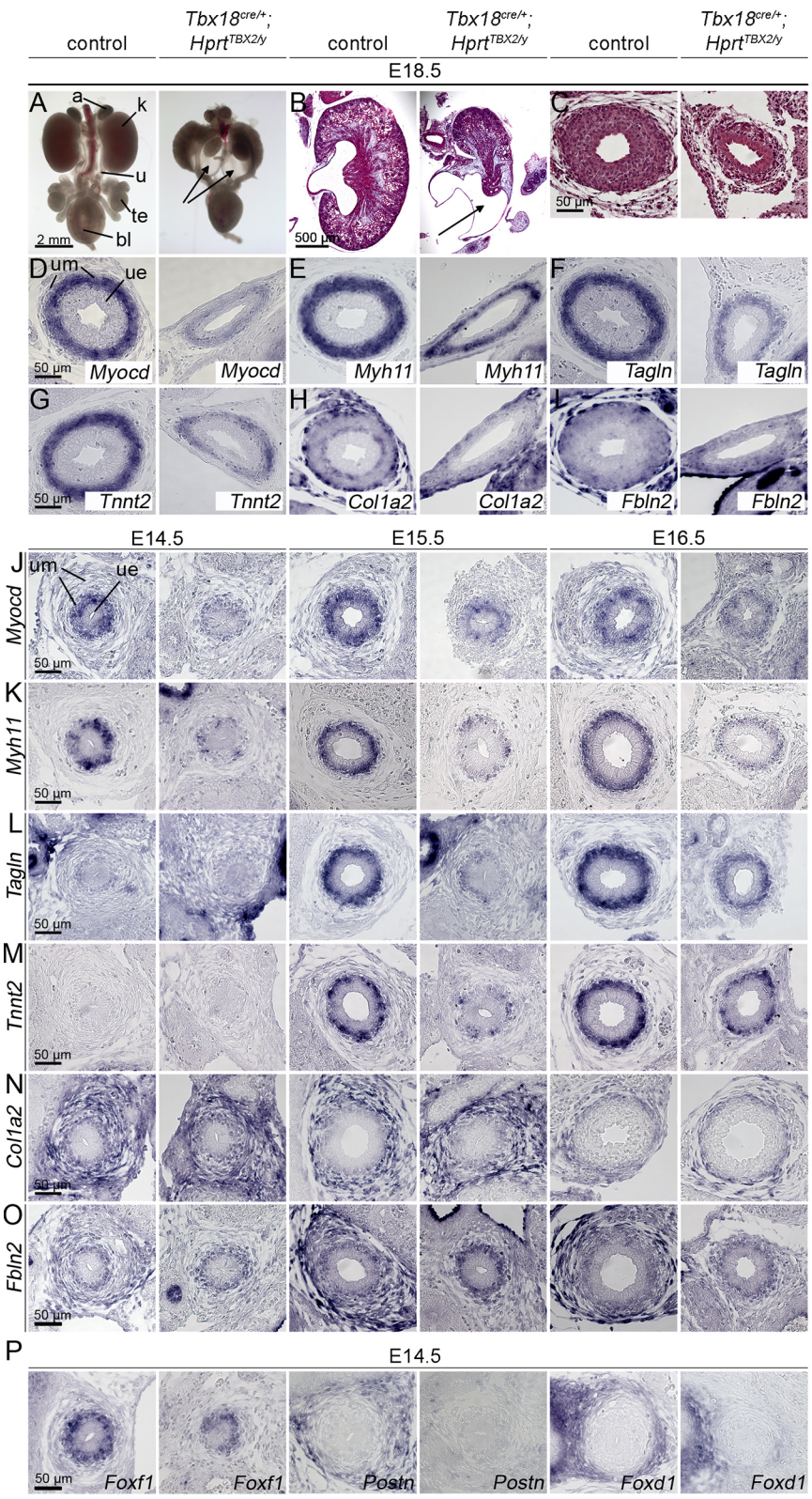

Fig. 5. *Tbx18*$^{cre/+}$;*Hprt*$^{TBX2/y}$ embryos develop uretero-pelvic junction obstruction and exhibit delayed and reduced SMC differentiation. (A) Morphology of whole urogenital systems of male E18.5 embryos reveals an enlarged pelvic space (arrows) in the mutant (n=10 out of 10) but not in the control (n=12 out of 12). (B,C) Hematoxylin and Eosin staining of sagittal sections of kidneys with the enlarged pelvic space (arrow) (B), and of transverse sections of the proximal ureter (C). (D-O) *In situ* hybridization analysis on proximal ureter sections at E18.5 (D-I) and at E14.5 to E16.5 (J-O) for expression of SMC markers (D-G,J-M) and *tunica adventitia* markers (H,I,N,O). (P) *In situ* hybridization analysis on transverse sections of the proximal ureter region at E14.5. a, adrenal; bl, bladder; k, kidney; te, testis; u, ureter; ue, ureteric epithelium; um, ureteric mesenchyme.

developmental programs. To date, the molecular functions of these genes in the development of the mammalian urinary system were not characterized. Here, we identified a crucial role for these transcriptional repressors in the development of SMCs, the cell type essential for the contractile peristaltic activity of the ureter tube. Our results suggest that TBX2/TBX3 mediate specific aspects of canonical WNT signaling function in this tissue by restricting outer adventitial programs and supporting SMC differentiation in the inner region. Molecularly, this is achieved by regulation of BMP, and possibly of WNT and CXCL12 signaling (Fig. 7).

Development (2018) 145, dev171827. doi:10.1242/dev.171827

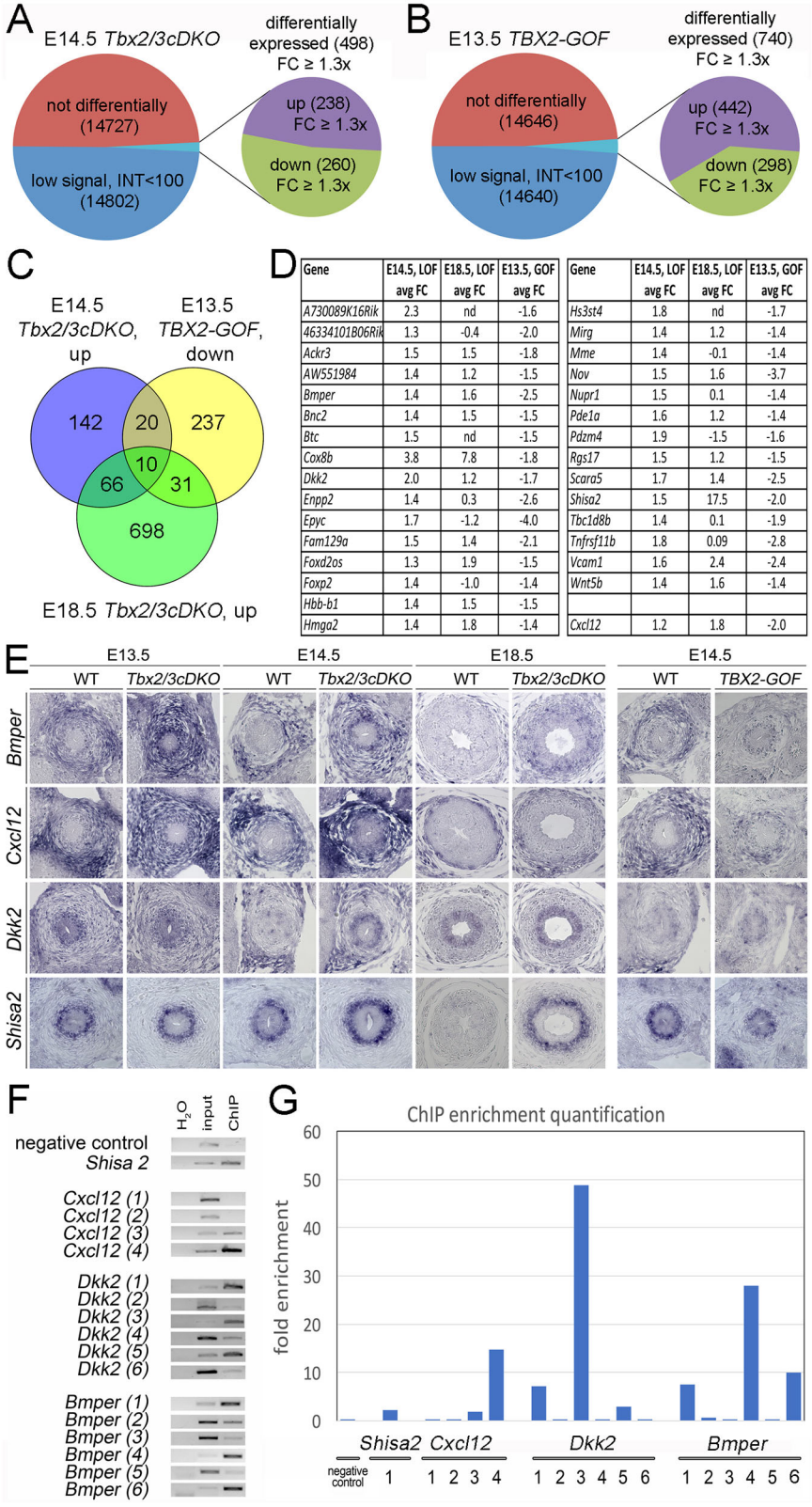

Gene	E14.5, LOF avg FC	E18.5, LOF avg FC	E13.5, GOF avg FC
A730089K16Rik	2.3	nd	-1.6
46334101B06Rik	1.3	-0.4	-2.0
Ackr3	1.5	1.5	-1.8
AW551984	1.4	1.2	-1.5
Bmper	1.4	1.6	-2.5
Bnc2	1.4	1.5	-1.5
Btc	1.5	nd	-1.5
Cox8b	3.8	7.8	-1.8
Dkk2	2.0	1.2	-1.7
Enpp2	1.4	0.3	-2.6
Epyc	1.7	-1.2	-4.0
Fam129a	1.5	1.4	-2.1
Foxd2os	1.3	1.9	-1.5
Foxp2	1.4	-1.0	-1.4
Hbb-b1	1.4	1.5	-1.5
Hmga2	1.4	1.8	-1.4

Gene	E14.5, LOF avg FC	E18.5, LOF avg FC	E13.5, GOF avg FC
Hs3st4	1.8	nd	-1.7
Mirg	1.4	1.2	-1.4
Mme	1.4	-0.1	-1.4
Nov	1.5	1.6	-3.7
Nupr1	1.5	0.1	-1.4
Pde1a	1.6	1.2	-1.4
Pdzm4	1.9	-1.5	-1.6
Rgs17	1.5	1.2	-1.5
Scara5	1.7	1.4	-2.5
Shisa2	1.5	17.5	-2.0
Tbc1d8b	1.4	0.1	-1.9
Tnfrsf11b	1.8	0.09	-2.8
Vcam1	1.6	2.4	-2.4
Wnt5b	1.4	1.6	-1.4
Cxcl12	1.2	1.8	-2.0

Fig. 6. Comparative transcriptome analysis of *Tbx2/Tbx3* loss- and gain-of-function ureters identifies genes regulated by TBX2/TBX3. (A,B) The Venn diagrams display the transcriptional outcomes of *Tbx2/Tbx3* loss of function (A) and *Tbx18*$^{cre/+}$;*Hprt*$^{TBX2/y}$ (*TBX2-GOF*; B) ureters at E14.5 and E13.5, respectively. (C) Intersection of transcripts upregulated in *Tbx2/3cDKO* ureters at E14.5, downregulated in *TBX2-GOF* ureters at E13.5, and upregulated in *Tbx2/3cDKO* ureters at E18.5. (D) List of 30 genes in common between E14.5 *Tbx2/3cDKO* (LOF) and E13.5 *TBX2-GOF* ureters. (E) *In situ* hybridization analysis of expression of *Bmper*, *Cxcl12*, *Dkk2* and *Shisa2*, which are repressed by TBX2/TBX3 in the inner layer of the UM. WT, wild-type control. (F) ChIP validation of peak regions shown in Fig. S14 and Table S14. H_2O refers to negative PCR controls without genomic DNA. Input refers to a PCR with chromatin DNA prior to immunoprecipitation, ChIP to PCR with chromatin obtained by immunoprecipitation with anti-TBX2 antibodies on E14.5 ureters. (G) Quantification of ChIP enrichment of identified peak regions in the four tested genes. FC, fold change; INT, expression intensity.

TBX2 and TBX3 mediate part of the function of canonical WNT signaling in the UM

SMCs provide the main support for the structure and the contractile activity of many tubular organs. Expression of many of the genes that characterize the SMC phenotype is under control of serum response factor (SRF), which recognizes cognate binding sites in the promotors of these genes and activates gene expression in combination with strong transcriptional activators such as MYOCD (Coletti et al., 2016; Miano, 2015). Expression and activity of SRF and MYOCD is regulated by a variety of intrinsic and extrinsic signals that reflect the heterogeneous developmental origin of this cell population. In the vascular system, NOTCH,

Development (2018) 145, dev171827. doi:10.1242/dev.171827

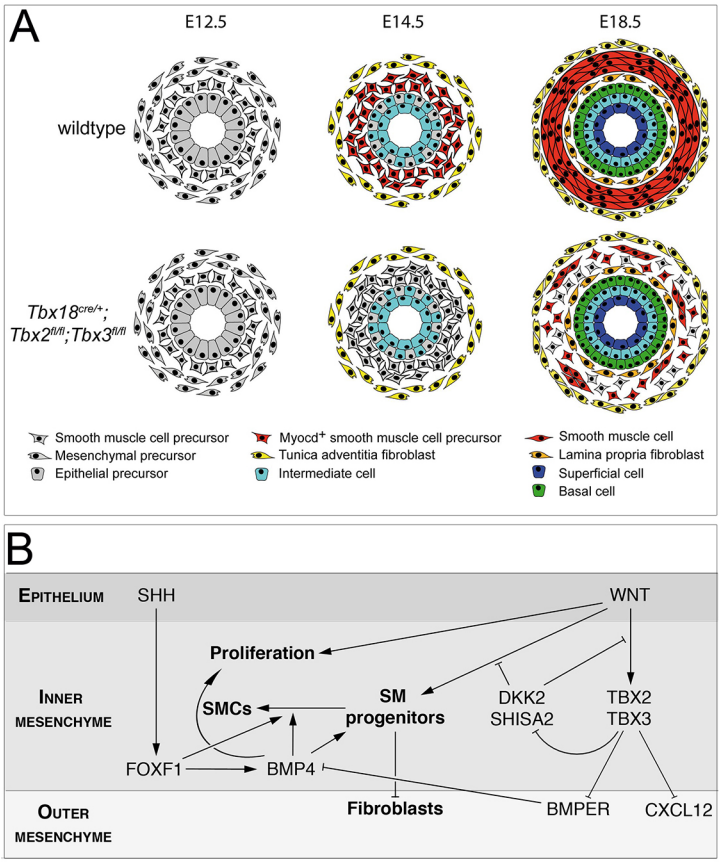

Fig. 7. Model of how TBX2 and TBX3 regulate various signaling pathways to ensure normal patterning and SMC differentiation of the UM. (A) Scheme of patterning and differentiation of the UM. In the wild type, the UM is subdivided into an inner layer with condensed cells with a rhomboid-shape, and an outer layer with fibroblast-like cells that are loosely associated, at E12.5. At E14.5, the inner layer becomes MYOCD positive and the outer layer expresses adventitial markers. At E18.5, three mesenchymal cell layers are established: the inner *lamina propria*, the middle *tunica muscularis* and the outer *tunica adventitia*. In *Tbx2/3cDKO* ureters, SMC progenitors are established in the inner mesenchymal layer at E12.5 but these cells subsequently only partly activate MYOCD expression in a delayed fashion to form dispersed clusters of contractile SMCs at E18.5. (B) Scheme of the molecular function of TBX2 and TBX3 in UM patterning and differentiation. WNT signaling induces SMC progenitors in the inner region of the UM, on which the SHH-FOXF1-BMP4 signaling axis acts to promote SMC differentiation. TBX2 and TBX3 support this process by maintaining WNT signaling through repression of the WNT antagonists DKK2 and SHISA2, by maintaining BMP4 signaling through repression of the BMP antagonist BMPER, and by repression of CXCL12.

TGFβ and platelet-derived growth factor have been characterized as main drivers of SMC differentiation, whereas in visceral tubes, SHH, BMPs and WNTs are predominant (Cohen et al., 2009; Itäranta et al., 2006; Mack, 2011; Shi and Chen, 2016; Trowe et al., 2012). The molecular targets of these signals, particularly of WNTs, as well as their interactions have remained poorly understood. Our previous work showed that WNT signaling is necessary and sufficient to subdivide the homogenous UM in a radial fashion by inducing cells in the vicinity of the epithelium (i.e. close to the source of the signal) to restrict to the SMC lineage (Trowe et al., 2012). Our expression analysis, in combination with conditional loss- and gain-of-function experiments, suggest that *Tbx2* and *Tbx3* are targets of this pathway and mediate some of its patterning and differentiation functions in the UM.

Our expression analysis showed that *Tbx2* and *Tbx3* are co-expressed in the inner layer of the UM from E12.5 to around E16.5. This pattern coincides with that of *Axin2*, a read-out of canonical WNT signaling (Jho et al., 2002; Trowe et al., 2012). Loss of *Ctnnb1* abolished the mesenchymal expression of *Tbx2* and *Tbx3* in the ureter whereas a stabilized version of CTNNB1 was sufficient to induce ectopic expression of the two genes, collectively indicating that canonical WNT signaling regulates (co-)expression of *Tbx2* and *Tbx3* in the UM. It is noteworthy that expression of *Tbx2* and *Tbx3* at other embryonic sites is regulated by other signals, including BMPs (Behesti et al., 2006; Ma et al., 2005; Zirzow et al., 2009) and SHH (Lüdtke et al., 2016), indicating that the regulatory landscape for ureter expression of *Tbx2* and *Tbx3* is tissue specific.

Combined loss of *Tbx2* and *Tbx3* in the UM did not affect proliferation and resulted in the formation of a ureter of normal length showing that the pro-proliferative aspect of WNT signaling on mesenchymal progenitors is independent of these two factors. This comes as a surprise because in other *in vivo* and *in vitro* settings TBX2 and TBX3 repress cell cycle inhibitors to ensure proliferative expansion of progenitors (Jacobs et al., 2000; Lüdtke et al., 2013; Prince et al., 2004). It is conceivable that WNT signaling directly regulates cell cycle activators, such as *Ccnd1* and *Myc*, as previously shown (Trowe et al., 2012), or employs as yet unknown transcription factors in the regulation of cell cycle progression.

Tbx2/3cDKO ureters displayed an expansion of expression of genes encoding ECM proteins, particularly collagens and fibulins, into the inner SMC layer of the ureteric wall, and ectopic expression of TBX2 was sufficient to repress expression of some of these genes in the outer layer. However, a clearly demarcated outer *tunica adventitia* with tangentially oriented fibroblast-like cells that expressed markers such as *Dpt* and *Postn* was established in *Tbx2/3cDKO* ureters. Hence, TBX2/TBX3 do not mediate all patterning functions of WNT signaling in the UM, but are required to suppress a particular adventitial subprogram, namely the deposition of ECM in the inner layer of the UM.

Possibly connected with this phenotypic difference is the finding that SMCs are not absent in *Tbx2/3cDKO* ureters but are dispersed, severely reduced in number and abnormally differentiated shortly before birth. Importantly, inner mesenchymal cells acquired a typical rhomboid shape, appeared condensed and expressed markers such as *Foxf1* and *Axin2* in the mutant at E14.5, compatible with the notion that SMC progenitors have been established. These SMC progenitors are likely to maintain their ability to produce ECM while being at least partially able to initiate the SMC differentiation program, similar to myofibroblasts associated with fibrotic disease states. Consequently, the *Tbx2/3cDKO* ureter can still withstand the hydrostatic pressure of the urine and does not dilate. In contrast, in *Ctnnb1*-deficient ureters

Development (2018) 145, dev171827. doi:10.1242/dev.171827

SMC progenitors are not established leading to complete absence of mature SMCs at birth and dilatation after onset of urine production in the fetal kidney (Trowe et al., 2012). Expansion of the adventitial fates to the inner mesenchymal region in these mutants may therefore simply reflect the default state of differentiation in the complete absence of SMC progenitors.

Although other (direct) targets of canonical WNT signaling in the UM have not been identified, molecular marker analysis of *Ctnnb1*-deficient ureters provided evidence for additional WNT-dependent factors possibly involved in SMC specification. Expression of *Tbx18* and *Sox9*, transcription factor genes required for the specification and SMC differentiation of the UM (Airik et al., 2006, 2010), respectively, were absent at E12.5, whereas at E14.5 expression of *Gata2*, *Tcf21* and *Tshz3* was lost. Moreover, expression of the SHH target gene, *Ptch1* and its mediator *Bmp4* was completely extinguished at this stage (Trowe et al., 2012). This indicates that WNT signaling maintains a set of crucial transcriptional regulators as well as the SHH-FOXF1-BMP4 regulatory axis independently of *Tbx2/Tbx3*, and that this could at least partly account for the lack of SMC specification and the more severe phenotype associated with its loss in the ureter.

Although misexpression of a stabilized version of CTNNB1 in the UM was sufficient to induce ectopic formation of SMC progenitors (Trowe et al., 2012), widespread and premature expression of TBX2 performed here did not; this is further evidence that TBX2/TBX3 acts downstream in a subprogram of SMC differentiation once progenitors are induced. In fact, misexpression of TBX2 resulted in a lack of SMC differentiation, revealing crucial temporal regulation for onset of expression after the progenitors are established. Although ectopic TBX2 did not affect the major signaling pathways, we found reduced expression of *Foxf1*, an essential downstream mediator of SHH signaling in SMC differentiation (Bohnenpoll et al., 2017b). Intriguingly, the *Foxf1/Foxf2* locus harbors a regulatory element bound and activated by TBX5 (Hoffmann et al., 2014). Because TBX2 and TBX3 can bind to the same DNA elements as TBX5 (Habets et al., 2002), it is conceivable that overexpressed TBX2 directly represses transcription of *Foxf1* and *Foxf2* upon binding to this element, thus compromising SMC differentiation.

Ideally, we would further substantiate our conclusion that TBX2/TBX3 mediate part of WNT signaling in the UM with a genetic rescue experiment. Unfortunately, this experiment is technically unfeasible at present because $Tbx18^{cre}$-mediated misexpression of TBX2 in the UM leads to SMC inhibition. An $Axin2^{creERT2}$ line would permit TBX2 expression in SMC progenitors but, as this line is itself under control of WNT signaling (Bohnenpoll et al., 2017b; van Amerongen et al., 2012), it cannot be activated when WNT signaling is inhibited as would be required for the rescue experiment.

TBX2 and TBX3 regulate specific signaling pathways in the UM

Our global analysis of transcriptional changes identified four genes that were both upregulated when *Tbx2/Tbx3* were inactivated and downregulated when enhanced TBX2 expression was forced into the UM. Compatible with the notion that they represent direct targets of TBX2/TBX3 transcriptional repression, they also featured productive TBX2/TBX3 binding peaks in their regulatory regions. The nature of the encoded proteins in combination with the observed molecular changes suggest that TBX2/TBX3 regulate SMC development largely by repressing *Bmper* to maintain BMP signaling. Repression of CXL12 signaling and maintenance of WNT signaling may present additional mediators of its function to permit functional SMCs.

Dkk2 encodes a member of a small family of secreted glycoproteins that inhibit WNT signaling by binding to the WNT co-receptors LRP5/6 and KREMEN (Mao et al., 2002, 2001). *Shisa2* encodes a member of a family of transmembrane proteins that trap WNT and FGF receptors in the endoplasmatic reticulum and prevent their maturation (Yamamoto et al., 2005). Both *Dkk2* and *Shisa2* were expressed in the inner layer of the UM in wild-type embryos at E13.5 and were subsequently downregulated (*Dkk2*) or maintained at low levels (*Shisa2*) compatible with the notion that they are involved in lowering the levels of WNT and possibly FGF signaling in this region at early stages. *Dkk2* was upregulated in *Tbx2/3cDKO* ureters at E14.5, but not at E18.5. In contrast, *Shisa2* was maintained at high levels even at E18.5. Surprisingly, at E14.5 expression of *Axin2*, a bona fide target of canonical WNT signaling, and of the FGF target *Etv4* (Mao et al., 2009), was unchanged in *Tbx2/3cDKO* embryos. This suggests that changes in the activities of these pathways are not present or are too small to be detected at this stage. Alternatively, *Axin2* and *Etv4* may not be faithful read-outs of the activity of these pathways in this context.

In a recent report on the molecular function of *Tbx2* and *Tbx3* in the pulmonary mesenchyme, *Frzb*, a secreted frizzled-related protein that competitively inhibits WNT binding to frizzled receptors, and *Shisa3* were identified as direct functional targets of TBX2/TBX3 in this tissue (Lüdtke et al., 2016). This adds to the notion that in some developmental contexts TBX2 and TBX3 maintain WNT signaling at high levels by repressing members of various families of WNT antagonists.

Although our data do not clearly indicate altered WNT signaling in developing *Tbx2/3cDKO* ureters, expression of the bona fide targets of BMP signaling *Id2* and *Id4* (Hollnagel et al., 1999; Liu and Harland, 2003) was clearly downregulated in the inner mesenchymal layer of *Tbx2/3cDKO* ureters at E14.5. This correlated with increased expression of the BMP antagonist gene *Bmper* (Moser et al., 2003), arguing that ectopic BMPER accounts for reduced BMP4 signaling. Interestingly, expression of *Bmp4* was strongly upregulated indicating a compensatory feedback mechanism. We found that *Foxf1* was also severely downregulated in the *Tbx2/3cDKO* ureters, suggesting a possible role of BMP4 signaling as an activator of *Foxf1* transcription. Alternatively, reduced SHH or WNT signaling input may have lowered *Foxf1* expression (Bohnenpoll et al., 2017b). As FOXF1 and BMP4 are both independently required for SMC differentiation in the ureter (Bohnenpoll et al., 2017b; Mamo et al., 2017), we suggest that their reduced expression and activity, respectively, largely accounts for the delayed and reduced onset of SMC differentiation in *Tbx2/3cDKO* ureters.

Notably, BMP4 signaling in the UE was not affected in *Tbx2/3cDKO* embryos. The expression level of *Id2* was normal and urothelial differentiation was unchanged. It is possible that urothelial differentiation requires lower levels of BMP4 than the mesenchyme (Bohnenpoll et al., 2017b). Alternatively, reduced expression of *Foxf1* and of BMP4 signaling may combinatorially enhance the mesenchymal defects, as discussed.

Our analysis also showed that TBX2/TBX3 are both required and sufficient to repress expression of *Cxcl12* in the inner layer of the UM. CXCL12 is a chemokine that mediates its effects by binding to CXCR4 and CXCR7 (ACKR3) (Balabanian et al., 2005; Burns et al., 2006). CXCL12 has a well-established role as a chemoattractant for numerous cell types, most prominently immune cells, but also circulating fibroblasts (Guyon, 2014). The latter may contribute in some organ settings to fibrosis by depositing collagens (Phillips et al.,

Development (2018) 145, dev171827. doi:10.1242/dev.171827

2004). A number of reports indicate a more direct involvement of CXCL12 in control of ECM deposition, possibly by conversion of resident fibroblasts to myofibroblasts (Jackson et al., 2017; Rodriguez-Nieves et al., 2016; Tan et al., 2017). Although the role of CXCL12/CXCR4/7 signaling in the ureter has not been analyzed, the above reports suggest that expanded CXCL12 signaling in *Tbx2/3cDKO* ureters contributes in some way to the ectopic deposition of ECM in the inner layer of the UM.

Together, our analysis reveals a crucial role for the T-box transcriptional repressors TBX2 and TBX3 in regulating the temporal and spatial activity of at least three different signaling pathways to assure the progression of SMC progenitors to fully differentiated contractile SMCs in the ureter (Fig. 7). Whether TBX2 and TBX3 play a similar role in the development of other visceral or vascular SMCs remains to be explored.

MATERIALS AND METHODS

Mouse strains and husbandry

The mouse alleles employed have all previously been described: a loss-of-function allele of *Tbx18* generated by insertion of the *cre* gene into the start codon [$Tbx18^{tm4(cre)Akis}$; synonym: $Tbx18^{cre}$] (Trowe et al., 2010); floxed loss-of-function lines for *Tbx2* ($Tbx2^{tm2.2Vmc}$; synonym: $Tbx2^{fl}$) (Wakker et al., 2010), *Tbx3* ($Tbx3^{tm3.2Moon}$; synonym: $Tbx3^{fl}$) (Frank et al., 2013), β-catenin ($Ctnnb1^{tm2Kem}$; synonym: $Ctnnb1^{fl}$) (Brault et al., 2001) and *Smo* (Smo^{tm2Amc}; synonym: Smo^{fl}) (Long et al., 2001); a floxed gain-of-function allele of β-catenin [$Ctnnb1^{tm1Mmt}$; synonym: $Ctnnb1^{(ex3)fl}$] (Harada et al., 1999); the reporter line $Gt(ROSA)26Sor^{tm4(ACTB-tdTomato,-EGFP)Luo}$ (synonym: $Rosa26^{mTmG}$) (Muzumdar et al., 2007); and an allele with insertion of the human *TBX2* gene at the *Hprt* locus [$Hprt^{tm2(CAG-TBX2,-EGFP)Akis}$; synonym: $Hprt^{TBX2}$] (Singh et al., 2012). All were maintained on an outbred (NMRI) background.

$Tbx18^{cre/+};Tbx2^{fl/fl};Tbx3^{fl/fl}$ embryos were generated by mating $Tbx18^{cre/+};Tbx2^{fl/+};Tbx3^{fl/+}$ males with $Tbx2^{fl/fl};Tbx3^{fl/fl};R26^{mTmG/mTmG}$ females. To generate embryos conditionally misexpressing human *TBX2* or stabilized *Ctnnb1*, $Tbx18^{cre/+}$ males were mated with $Hprt^{TBX2/TBX2}$ or $Ctnnb1^{(ex3)fl/(ex3)fl}$ females, respectively. *Cre*-negative littermates were used as controls. For timed pregnancies, vaginal plugs detected in the morning after mating were designated as E0.5 at noon.

All animal work conducted for this study was approved by the Niedersächsisches Landesamt für Verbraucherschutz und Lebensmittelsicherheit (permit number AZ33.12-42502-04-13/1356) and was performed at the central animal laboratory of the Medizinische Hochschule Hannover according to European and German legislation (2010/63/EU and TierSchG).

Organ cultures and video documentation

Ureters for explant cultures were dissected in L-15 Leibovitz medium (Biochrom). Ureters isolated from the embryo were explanted on 0.4 µm polyester membrane Transwell supports (Corning) and cultured at the air-liquid interface with DMEM/F12 (Gibco) supplemented with 10% fetal calf serum (Biochrom), 1× Penicillin/Streptomycin, 1× Pyruvate and 1× Glutamax (all from Gibco) in a humidified incubator with 5% CO_2 at 37°C. Medium was refreshed every second day.

To document the contractile behavior of ureter explants, culture plates were removed from the incubator and imaged for 1 min at room temperature using a Leica DMI6000B microscope. The contraction frequency was expressed as the number of full proximal-to-distal contractions per minute. Individual contraction intensities were defined as the difference between relaxed and contracted width divided by the relaxed width of the ureter. The overall contraction intensity was defined as the average of proximal, medial and distal contraction provided as a percentage. All movies were processed and analyzed using ImageJ software (Schneider et al., 2012).

Histological and immunohistochemical analyses

Embryos, urogenital systems and ureter explants were fixed in 4% paraformaldehyde, paraffin-embedded and sectioned at 5 µm. Sections were stained with Hematoxylin and Eosin according to standard procedures.

Immunofluorescence staining was performed on 5-µm-thick paraffin sections using the following primary antibodies: polyclonal rabbit-anti-TBX2 (1:500; 07-318, Millipore), polyclonal goat-anti-TBX3 (1:500; sc-31656, Santa Cruz), polyclonal rabbit-anti-KRT5 (1:250; PRB-160P-100, Covance), polyclonal rabbit-anti-ΔNP63 (1:250; 619001, BioLegend), monoclonal mouse-anti-UPK1B (1:250; WH0007348M2, Sigma-Aldrich), polyclonal rabbit-anti-TAGLN (1:200; ab14106, Abcam), polyclonal FITC-conjugated rabbit anti-ACTA2 (1:200; F3777, Sigma-Aldrich) and monoclonal mouse-anti-BrdU (1:250; 1170376, Roche).

Fluorescent staining was performed using the following secondary antibodies: biotinylated goat anti-rabbit IgG (1:250; 111065033, Dianova), biotinylated donkey anti-goat IgG (1:250; 705-065-003, Dianova), biotinylated goat-anti-mouse IgG (1:250; 115-065-003, Jackson ImmunoResearch), Alexa 488-conjugated goat anti-rabbit IgG (1:500; A11034, Molecular Probes) and Alexa 555-conjugated goat anti-mouse IgG (1:500; A21422, Molecular Probes). The signals of TBX2, TBX3, ΔNP63 and BrdU were amplified using the Tyramide Signal Amplification system (Perkin Elmer). For antigen retrieval, paraffin sections were deparaffinized, pressure-cooked for 20 min in antigen unmasking solution (Vector Laboratories), treated with 3% H_2O_2/PBS for blocking of endogenous peroxidases, washed in PBST (0.05% Tween-20 in PBS) and incubated in TNB Blocking Buffer (Perkin Elmer). Sections were then incubated with primary antibodies at 4°C overnight. Nuclei were stained with 4′,6-diamidino-2-phenylindole (DAPI). At least three specimens of each genotype were used for each analysis.

Cellular assays

In vivo cell proliferation rates of E12.5 and E14.5 *cre*-negative (control) and $Tbx18^{cre/+};Tbx2^{fl/fl};Tbx3^{fl/fl}$ ureters were assayed by detection of incorporated BrdU on 5-µm-thick sections (Bussen et al., 2004). Twelve sections of each specimen (n=5) were analyzed. The BrdU labeling index was defined as the number of BrdU-positive nuclei relative to the total number of nuclei detected by DAPI counterstaining in histologically defined compartments of the ureter. Statistical analysis was performed using the two-tailed Student's t-test. Values are indicated as mean±s.d. $P<0.05$ was considered significant. Apoptosis in tissues was assessed by TUNEL assay using the ApopTag Plus Fluorescein In Situ Apoptosis Detection Kit (Chemicon) on 5-µm-thick paraffin sections.

In situ hybridization analysis

Non-radioactive *in situ* hybridization analysis of gene expression was performed on 10-µm-thick paraffin sections of the proximal and distal ureter using digoxigenin-labeled antisense riboprobes as described previously (Moorman et al., 2001). At least three specimens of each genotype were used for each analysis.

Microarray analysis

Two independent pools each of control and mutant ureters were used for microarray analysis. Pool sizes were as follows: 20 ureters from E14.5 *cre*-negative and $Tbx18^{cre/+};Tbx2^{fl/fl};Tbx3^{fl/fl}$ embryos; 12, 24, 12 and 18 ureters from E18.5 male and female *cre*-negative, male and female $Tbx18^{cre/+};Tbx2^{fl/fl};Tbx3^{fl/fl}$ embryos, respectively; and 44 and 53 ureters from E13.5 male *cre*-negative and male $Tbx18^{cre/+};Hprt^{TBX2/y}$ embryos, respectively. Total RNA from each pool was extracted using peqGOLD RNApure (PeqLab) and subsequently processed by the Research Core Unit Transcriptomics of Hannover Medical School. Whole Mouse Genome Oligo v2 (4×44K) Microarrays were used for E18.5 $Tbx18^{cre/+};Tbx2^{fl/fl};Tbx3^{fl/fl}$ and E13.5 $Tbx18^{cre/+};Hprt^{TBX2/y}$ microarray analysis. 048306On1M_V2 microarrays were used for E14.5 $Tbx18^{cre/+};Tbx2^{fl/fl};Tbx3^{fl/fl}$ transcriptome analysis. Normalized expression data were filtered using Excel. Functional enrichment analysis for up- and downregulated genes was performed with DAVID 6.8 web-software (david.ncifcrf.gov) using default settings, and terms were selected based on P-value. P-values for the overlap of different gene sets were calculated using Fisher's exact test.

Chromatin immunoprecipitation (ChIP) analysis

ChIP was performed using the SimpleChIP Plus Enzymatic Chromatin IP Kit (Magnetic Beads) (9005, Cell Signaling). Approximately 100 dissected E14.5 ureters were treated according to the manufacturer's instructions. Single-cell suspensions were generated using a Minilys homogenizer with mixed 1.4/2.8 mm ceramic beads (Peqlab). The DNA-containing supernatants were incubated overnight with a rabbit anti-TBX2 (1:25; 07-318, Merck Millipore) antibody and collected on ProteinG Magnetic Beads (9006, NEB) with a magnetic MiniMACS Separator (130-042-102, Miltenyi Biotec). Quantification of ChIP-enrichment over 2% input control was performed by semi-quantitative PCR according to the manufacturer's instructions.

Image documentation

Sections were imaged using a Leica DM5000 microscope with Leica DFC300FX digital camera or a Leica DMI6000B microscope with Leica DFC350FX digital camera. All images were then processed in Adobe Photoshop CS4.

Acknowledgements

We thank Rolf Kemler for the *Ctnnb1* floxed mouse line. Microarray data used in this publication were generated by the Research Core Unit Genomics (RCUG) at Hannover Medical School.

Competing interests

The authors declare no competing or financial interests.

Author contributions

Conceptualization: N.A., A.K.; Methodology: N.A., C.R., M.-O.T., A.K.; Software: M.-O.T.; Validation: M.-O.T., T.H.L.; Formal analysis: N.A., C.R., M.-O.T., M.K., T.H.L.; Investigation: N.A., C.R., M.-O.T., M.K., T.H.L., A.K.; Resources: M.M.T., V.M.C., A.M., A.K.; Data curation: N.A., M.-O.T., A.K.; Writing - original draft: N.A., A.K.; Writing - review & editing: C.R., M.-O.T., M.K., T.H.L., M.M.T., V.M.C., A.M., A.K.; Visualization: N.A., M.-O.T., M.K., T.H.L., A.K.; Supervision: C.R., A.K.; Project administration: A.K.; Funding acquisition: A.K.

Funding

This work was supported by grants from the Deutsche Forschungsgemeinschaft (DFG KI728/8-2, KI728/10-1 to A.K.). N.A. was supported by the Hannover Biomedical Research School (HBRS) and the MD/PhD program Molecular Medicine.

Data availability

Microarray data have been deposited in GEO under accession number GSE122561.

Supplementary information

Supplementary information available online at
http://dev.biologists.org/lookup/doi/10.1242/dev.171827.supplemental

References

Airik, R., Bussen, M., Singh, M. K., Petry, M. and Kispert, A. (2006). Tbx18 regulates the development of the ureteral mesenchyme. *J. Clin. Invest.* **116**, 663-674.

Airik, R., Trowe, M.-O., Foik, A., Farin, H. F., Petry, M., Schuster-Gossler, K., Schweizer, M., Scherer, G., Kist, R. and Kispert, A. (2010). Hydroureternephrosis due to loss of Sox9-regulated smooth muscle cell differentiation of the ureteric mesenchyme. *Hum. Mol. Genet.* **19**, 4918-4929.

Balabanian, K., Lagane, B., Infantino, S., Chow, K. Y. C., Harriague, J., Moepps, B., Arenzana-Seisdedos, F., Thelen, M. and Bachelerie, F. (2005). The chemokine SDF-1/CXCL12 binds to and signals through the orphan receptor RDC1 in T lymphocytes. *J. Biol. Chem.* **280**, 35760-35766.

Baskin, L. S., Hayward, S. W., Young, P. and Cunha, G. R. (1996). Role of mesenchymal-epithelial interactions in normal bladder development. *J. Urol.* **156**, 1820-1827.

Behesti, H., Holt, J. K. L. and Sowden, J. C. (2006). The level of BMP4 signaling is critical for the regulation of distinct T-box gene expression domains and growth along the dorso-ventral axis of the optic cup. *BMC Dev. Biol.* **6**, 62.

Bohnenpoll, T. and Kispert, A. (2014). Ureter growth and differentiation. *Semin. Cell Dev. Biol.* **36**, 21-30.

Bohnenpoll, T., Bettenhausen, E., Weiss, A.-C., Foik, A. B., Trowe, M.-O., Blank, P., Airik, R. and Kispert, A. (2013). Tbx18 expression demarcates multipotent precursor populations in the developing urogenital system but is exclusively required within the ureteric mesenchymal lineage to suppress a renal stromal fate. *Dev. Biol.* **380**, 25-36.

Bohnenpoll, T., Feraric, S., Nattkemper, M., Weiss, A.-C., Rudat, C., Meuser, M., Trowe, M.-O. and Kispert, A. (2017a). Diversification of cell lineages in ureter development. *J. Am. Soc. Nephrol.* **28**, 1792-1801.

Bohnenpoll, T., Wittern, A. B., Mamo, T. M., Weiss, A.-C., Rudat, C., Kleppa, M.-J., Schuster-Gossler, K., Wojahn, I., Lüdtke, T. H.-W., Trowe, M.-O. et al. (2017b). A SHH-FOXF1-BMP4 signaling axis regulating growth and differentiation of epithelial and mesenchymal tissues in ureter development. *PLoS Genet.* **13**, e1006951.

Brault, V., Moore, R., Kutsch, S., Ishibashi, M., Rowitch, D. H., McMahon, A. P., Sommer, L., Boussadia, O. and Kemler, R. (2001). Inactivation of the beta-catenin gene by Wnt1-Cre-mediated deletion results in dramatic brain malformation and failure of craniofacial development. *Development* **128**, 1253-1264.

Burns, J. M., Summers, B. C., Wang, Y., Melikian, A., Berahovich, R., Miao, Z., Penfold, M. E., Sunshine, M. J., Littman, D. R., Kuo, C. J. et al. (2006). A novel chemokine receptor for SDF-1 and I-TAC involved in cell survival, cell adhesion, and tumor development. *J. Exp. Med.* **203**, 2201-2213.

Bussen, M., Petry, M., Schuster-Gossler, K., Leitges, M., Gossler, A. and Kispert, A. (2004). The T-box transcription factor Tbx18 maintains the separation of anterior and posterior somite compartments. *Genes Dev.* **18**, 1209-1221.

Campbell, C., Goodrich, K., Casey, G. and Beatty, B. (1995). Cloning and mapping of a human gene (TBX2) sharing a highly conserved protein motif with the Drosophila omb gene. *Genomics* **28**, 255-260.

Chapman, D. L., Garvey, N., Hancock, S., Alexiou, M., Agulnik, S. I., Gibson-Brown, J. J., Cebra-Thomas, J., Bollag, R. J., Silver, L. M. and Papaioannou, V. E. (1996). Expression of the T-box family genes, Tbx1-Tbx5, during early mouse development. *Dev. Dyn.* **206**, 379-390.

Cohen, E. D., Ihida-Stansbury, K., Lu, M. M., Panettieri, R. A., Jones, P. L. and Morrisey, E. E. (2009). Wnt signaling regulates smooth muscle precursor development in the mouse lung via a tenascin C/PDGFR pathway. *J. Clin. Invest.* **119**, 2538-2549.

Coletti, D., Daou, N., Hassani, M., Li, Z. and Parlakian, A. (2016). Serum response factor in muscle tissues: from development to ageing. *Eur. J. Transl. Myol.* **26**, 6008.

Cunha, G. R., Young, P., Higgins, S. J. and Cooke, P. S. (1991). Neonatal seminal vesicle mesenchyme induces a new morphological and functional phenotype in the epithelia of adult ureter and ductus deferens. *Development* **111**, 145-158.

Douglas, N. C. and Papaioannou, V. E. (2013). The T-box transcription factors TBX2 and TBX3 in mammary gland development and breast cancer. *J. Mammary Gland Biol. Neoplasia* **18**, 143-147.

Douglas, N. C., Heng, K., Sauer, M. V. and Papaioannou, V. E. (2012). Dynamic expression of Tbx2 subfamily genes in development of the mouse reproductive system. *Dev. Dyn.* **241**, 365-375.

Frank, D. U., Emechebe, U., Thomas, K. R. and Moon, A. M. (2013). Mouse TBX3 mutants suggest novel molecular mechanisms for Ulnar-mammary syndrome. *PLoS ONE* **8**, e67841.

Glinka, A., Wu, W., Delius, H., Monaghan, A. P., Blumenstock, C. and Niehrs, C. (1998). Dickkopf-1 is a member of a new family of secreted proteins and functions in head induction. *Nature* **391**, 357-362.

Gonzalez, C. H., Herrmann, J. and Opitz, J. M. (1976). Studies of malformation syndromes of man XXXXIIB: mother and son affected with the ulnar-mammary syndrome type Pallister. *Eur. J. Pediatr.* **123**, 225-235.

Guyon, A. (2014). CXCL12 chemokine and its receptors as major players in the interactions between immune and nervous systems. *Front. Cell Neurosci.* **8**, 65.

Habets, P. E., Moorman, A. F., Clout, D. E., van Roon, M. A., Lingbeek, M., van Lohuizen, M., Campione, M. and Christoffels, V. M. (2002). Cooperative action of Tbx2 and Nkx2.5 inhibits ANF expression in the atrioventricular canal: implications for cardiac chamber formation. *Genes Dev.* **16**, 1234-1246.

Harada, N., Tamai, Y., Ishikawa, T., Sauer, B., Takaku, K., Oshima, M. and Taketo, M. M. (1999). Intestinal polyposis in mice with a dominant stable mutation of the beta-catenin gene. *EMBO J.* **18**, 5931-5942.

Harris, D. A., Zhao, Y., LaPar, D. J., Emaminia, A., Steidle, J. F., Stoler, M., Linden, J., Kron, I. L. and Lau, C. L. (2013). Inhibiting CXCL12 blocks fibrocyte migration and differentiation and attenuates bronchiolitis obliterans in a murine heterotopic tracheal transplant model. *J. Thorac. Cardiovasc. Surg.* **145**, 854-861.

Hoffmann, A. D., Yang, X. H., Burnicka-Turek, O., Bosman, J. D., Ren, X., Steimle, J. D., Vokes, S. A., McMahon, A. P., Kalinichenko, V. V. and Moskowitz, I. P. (2014). Foxf genes integrate tbx5 and hedgehog pathways in the second heart field for cardiac septation. *PLoS Genet.* **10**, e1004604.

Hollnagel, A., Oehlmann, V., Heymer, J., Rüther, U. and Nordheim, A. (1999). Id genes are direct targets of bone morphogenetic protein induction in embryonic stem cells. *J. Biol. Chem.* **274**, 19838-19845.

Ingham, P. W. and McMahon, A. P. (2001). Hedgehog signaling in animal development: paradigms and principles. *Genes Dev.* **15**, 3059-3087.

Iruela-Arispe, M. L. and Beitel, G. J. (2013). Tubulogenesis. *Development* **140**, 2851-2855.

Itäranta, P., Chi, L., Seppänen, T., Niku, M., Tuukkanen, J., Peltoketo, H. and Vainio, S. (2006). Wnt-4 signaling is involved in the control of smooth muscle cell

fate via Bmp-4 in the medullary stroma of the developing kidney. *Dev. Biol.* **293**, 473-483.

Ito, A., Asamoto, M., Hokaiwado, N., Takahashi, S. and Shirai, T. (2005). Tbx3 expression is related to apoptosis and cell proliferation in rat bladder both hyperplastic epithelial cells and carcinoma cells. *Cancer Lett.* **219**, 105-112.

Jackson, E. K., Zhang, Y., Gillespie, D. D., Zhu, X., Cheng, D. and Jackson, T. C. (2017). SDF-1alpha (stromal cell-derived factor 1alpha) induces cardiac fibroblasts, renal microvascular smooth muscle cells, and glomerular mesangial cells to proliferate, cause hypertrophy, and produce collagen. *J. Am. Heart Assoc.* **6**, e007253.

Jacobs, J. J. L., Keblusek, P., Robanus-Maandag, E., Kristel, P., Lingbeek, M., Nederlof, P. M., van Welsem, T., van de Vijver, M. J., Koh, E. Y., Daley, G. Q. et al. (2000). Senescence bypass screen identifies TBX2, which represses Cdkn2a (p19(ARF)) and is amplified in a subset of human breast cancers. *Nat. Genet.* **26**, 291-299.

Jho, E.-H., Zhang, T., Domon, C., Joo, C.-K., Freund, J.-N. and Costantini, F. (2002). Wnt/beta-catenin/Tcf signaling induces the transcription of Axin2, a negative regulator of the signaling pathway. *Mol. Cell. Biol.* **22**, 1172-1183.

Law, D. J., Gebuhr, T., Garvey, N., Agulnik, S. I. and Silver, L. M. (1995). Identification, characterization, and localization to chromosome 17q21-22 of the human TBX2 homolog, member of a conserved developmental gene family. *Mamm. Genome* **6**, 793-797.

Liu, K. J. and Harland, R. M. (2003). Cloning and characterization of Xenopus Id4 reveals differing roles for Id genes. *Dev. Biol.* **264**, 339-351.

Long, F., Zhang, X. M., Karp, S., Yang, Y. and McMahon, A. P. (2001). Genetic manipulation of hedgehog signaling in the endochondral skeleton reveals a direct role in the regulation of chondrocyte proliferation. *Development* **128**, 5099-5108.

Lu, J., Li, X. P., Dong, Q., Kung, H. F. and He, M. L. (2010). TBX2 and TBX3: the special value for anticancer drug targets. *Biochim. Biophys. Acta* **1806**, 268-274.

Lüdtke, T. H.-W., Farin, H. F., Rudat, C., Schuster-Gossler, K., Petry, M., Barnett, P., Christoffels, V. M. and Kispert, A. (2013). Tbx2 controls lung growth by direct repression of the cell cycle inhibitor genes Cdkn1a and Cdkn1b. *PLoS Genet.* **9**, e1003189.

Ludtke, T. H., Rudat, C., Wojahn, I., Weiss, A.-C., Kleppa, M.-J., Kurz, J., Farin, H. F., Moon, A., Christoffels, V. M. and Kispert, A. (2016). Tbx2 and Tbx3 act downstream of Shh to maintain canonical Wnt signaling during branching morphogenesis of the murine lung. *Dev. Cell* **39**, 239-253.

Ma, L., Lu, M. F., Schwartz, R. J. and Martin, J. F. (2005). Bmp2 is essential for cardiac cushion epithelial-mesenchymal transition and myocardial patterning. *Development* **132**, 5601-5611.

Mack, C. P. (2011). Signaling mechanisms that regulate smooth muscle cell differentiation. *Arterioscler. Thromb. Vasc. Biol.* **31**, 1495-1505.

Mamo, T. M., Wittern, A. B., Kleppa, M.-J., Bohnenpoll, T., Weiss, A.-C. and Kispert, A. (2017). BMP4 uses several different effector pathways to regulate proliferation and differentiation in the epithelial and mesenchymal tissue compartments of the developing mouse ureter. *Hum. Mol. Genet.* **26**, 3553-3563.

Mao, B., Wu, W., Li, Y., Hoppe, D., Stannek, P., Glinka, A. and Niehrs, C. (2001). LDL-receptor-related protein 6 is a receptor for Dickkopf proteins. *Nature* **411**, 321-325.

Mao, B., Wu, W., Davidson, G., Marhold, J., Li, M., Mechler, B. M., Delius, H., Hoppe, D., Stannek, P., Walter, C. et al. (2002). Kremen proteins are Dickkopf receptors that regulate Wnt/beta-catenin signalling. *Nature* **417**, 664-667.

Mao, J., McGlinn, E., Huang, P., Tabin, C. J. and McMahon, A. P. (2009). Fgf-dependent Etv4/5 activity is required for posterior restriction of Sonic Hedgehog and promoting outgrowth of the vertebrate limb. *Dev. Cell* **16**, 600-606.

Mendelsohn, C., Ruberte, E., LeMeur, M., Morriss-Kay, G. and Chambon, P. (1991). Developmental analysis of the retinoic acid-inducible RAR-beta 2 promoter in transgenic animals. *Development* **113**, 723-734.

Miano, J. M. (2015). Myocardin in biology and disease. *J. Biomed. Res.* **29**, 3-19.

Moorman, A. F., Houweling, A. C., de Boer, P. A. and Christoffels, V. M. (2001). Sensitive nonradioactive detection of mRNA in tissue sections: novel application of the whole-mount in situ hybridization protocol. *J. Histochem. Cytochem.* **49**, 1-8.

Moser, M., Binder, O., Wu, Y., Aitsebaomo, J., Ren, R., Bode, C., Bautch, V. L., Conlon, F. L. and Patterson, C. (2003). BMPER, a novel endothelial cell precursor-derived protein, antagonizes bone morphogenetic protein signaling and endothelial cell differentiation. *Mol. Cell. Biol.* **23**, 5664-5679.

Muzumdar, M. D., Tasic, B., Miyamichi, K., Li, L. and Luo, L. (2007). A global double-fluorescent Cre reporter mouse. *Genesis* **45**, 593-605.

Pallister, P. D., Herrmann, J. and Opitz, J. M. (1976). Studies of malformation syndromes in man XXXXII: a pleiotropic dominant mutation affecting skeletal, sexual and apocrine-mammary development. *Birth Defects Orig. Artic. Ser.* **12**, 247-254.

Papaioannou, V. E. (2014). The T-box gene family: emerging roles in development, stem cells and cancer. *Development* **141**, 3819-3833.

Phillips, R. J., Burdick, M. D., Hong, K., Lutz, M. A., Murray, L. A., Xue, Y. Y., Belperio, J. A., Keane, M. P. and Strieter, R. M. (2004). Circulating fibrocytes traffic to the lungs in response to CXCL12 and mediate fibrosis. *J. Clin. Invest.* **114**, 438-446.

Prince, S., Carreira, S., Vance, K. W., Abrahams, A. and Goding, C. R. (2004). Tbx2 directly represses the expression of the p21(WAF1) cyclin-dependent kinase inhibitor. *Cancer Res.* **64**, 1669-1674.

Rodriguez-Nieves, J. A., Patalano, S. C., Almanza, D., Gharaee-Kermani, M. and Macoska, J. A. (2016). CXCL12/CXCR4 axis activation mediates prostate myofibroblast phenoconversion through non-canonical EGFR/MEK/ERK signaling. *PLoS ONE* **11**, e0159490.

Schneider, C. A., Rasband, W. S. and Eliceiri, K. W. (2012). NIH Image to ImageJ: 25 years of image analysis. *Nat. Methods* **9**, 671-675.

Shi, N. and Chen, S.-Y. (2016). Smooth muscle cell differentiation: model systems, regulatory mechanisms, and vascular diseases. *J. Cell. Physiol.* **231**, 777-787.

Singh, R., Hoogaars, W. M., Barnett, P., Grieskamp, T., Rana, M. S., Buermans, H., Farin, H. F., Petry, M., Heallen, T., Martin, J. F. et al. (2012). Tbx2 and Tbx3 induce atrioventricular myocardial development and endocardial cushion formation. *Cell. Mol. Life Sci.* **69**, 1377-1389.

Tan, J., Tedrow, J. R., Nouraie, M., Dutta, J. A., Miller, D. T., Li, X., Yu, S., Chu, Y., Juan-Guardela, B., Kaminski, N. et al. (2017). Loss of Twist1 in the mesenchymal compartment promotes increased fibrosis in experimental lung injury by enhanced expression of CXCL12. *J. Immunol.* **198**, 2269-2285.

Trowe, M.-O., Shah, S., Petry, M., Airik, R., Schuster-Gossler, K., Kist, R. and Kispert, A. (2010). Loss of Sox9 in the periotic mesenchyme affects mesenchymal expansion and differentiation, and epithelial morphogenesis during cochlea development in the mouse. *Dev. Biol.* **342**, 51-62.

Trowe, M.-O., Airik, R., Weiss, A.-C., Farin, H. F., Foik, A. B., Bettenhausen, E., Schuster-Gossler, K., Taketo, M. M. and Kispert, A. (2012). Canonical Wnt signaling regulates smooth muscle precursor development in the mouse ureter. *Development* **139**, 3099-3108.

van Amerongen, R., Bowman, A. N. and Nusse, R. (2012). Developmental stage and time dictate the fate of Wnt/beta-catenin-responsive stem cells in the mammary gland. *Cell Stem Cell* **11**, 387-400.

Velardo, J. T. (1981). Histology of the ureter. In *The Ureter* (ed. H. Bergman), pp. 13-54. Springer-Verlag.

Wakker, V., Brons, J. F., Aanhaanen, W. T., van Roon, M. A., Moorman, A. F. and Christoffels, V. M. (2010). Generation of mice with a conditional null allele for Tbx2. *Genesis* **48**, 195-199.

Yamamoto, A., Nagano, T., Takehara, S., Hibi, M. and Aizawa, S. (2005). Shisa promotes head formation through the inhibition of receptor protein maturation for the caudalizing factors, Wnt and FGF. *Cell* **120**, 223-235.

Yu, J., Carroll, T. J. and McMahon, A. P. (2002). Sonic hedgehog regulates proliferation and differentiation of mesenchymal cells in the mouse metanephric kidney. *Development* **129**, 5301-5312.

Zirzow, S., Lüdtke, T. H.-W., Brons, J. F., Petry, M., Christoffels, V. M. and Kispert, A. (2009). Expression and requirement of T-box transcription factors Tbx2 and Tbx3 during secondary palate development in the mouse. *Dev. Biol.* **336**, 145-155.